2.5-D NUMERICAL MODELING ON FLOW AROUND A CYLINDER

B. Yulistiyanto[1)]

ABSTRACT

The equations for two-dimensional, horizontal flow are obtained by vertical depth-integration of the continuity and momentum equations. Consequently, the diffusion-dispersion terms are appeared, containing turbulent and "dispersion" stresses. A special emphasis was placed in elaborating the diffusion-dispersion terms. Turbulent stresses are expressed with the eddy viscosity concept; dispersion stresses are evaluated using velocity distributions along and across the curved streamlines. The differential equations are solved using MacCormack scheme. The numerical simulation was done for two runs; the expected alteration of the flow field around the cylinder is evident, notably the wake behind the cylinder.

For comparison, two similar runs were performed in a laboratory channel. The velocity vectors upstream from the cylinder and along its sides are in reasonably good agreement. However, very close to the cylinder, the simulation sometimes underpredicts the velocities. Downstream from the cylinder, agreement is satisfactory both inside and outside the wake. The flow depths at the center line both upstream and downstream from the cylinder are also in good agreement, however along the cylinder circumference, the simulated flow depths are lower than the observed ones.

INTRODUCTION

Flow around a cylinder positioned normal to the fixed-bed channel bottom represents a classical problem of fluvial hydraulics. It serves as a pre-study to flow over a moveable-bed bottom, which in turn is of importance to determine the local scour around the cylinder.

The objective of the present study is to gain a better understanding of the flow fields around the cylinder. This can be obtained either by mathematical modeling the flow fields and/or by performing extensive measurements around the cylinder.

Since the flow is highly three-dimensional, a three dimensional model would be the best; this is difficult task. We have opted for developing a 2.5-dimensional model by depth-averaging the velocity components and taking into acoount the depth-averaged turbulent stresses and the dispersion stresses. In the latter stresses, longitudinal and transversal velocity profiles are considered.

The governing Saint-Venant 2-D equations are derived from the Navier-Stokes equations. Of particular interest here are terms of the depth-averaged effective stresses. Similar forms of these equations have been presented- without given the derivation- before by Vreugdenhil, 1973, Flokstra ,1977, and Rodi, 1984, Khan and Chaudhry, 1992. This set of equations has - to our knowledge - never been applied to the geometrical situation of our problem.

In order to solve this system of equation, we have opted for the explicit finite-difference MacCormack scheme using forward and backward finite-differences. Three types of boundary conditions are imposed: mirror conditions along the walls, upstream inflow conditions and downstream stage. The latter conditions are based on the characteristic form of the flow equations. The MacCormack sceme has been succesfully used for different kind of flow with free surface (Fennema, R. J. and Chaudhry, M. H., 1986, Ballamudi, S. M. and Chaudhry, M. H., 1992)

An extensive measurement program was also launched (Yulistiyanto, 1997), but only the depth-averaged values are here used for our present study. No similar measurements - to our knowledge - are available in the literature.

GOVERNING EQUATIONS

The shallow-water two-dimensional equations are obtained by time averaging the Navier-Stokes equations and integrating these over the flow depth with some assumptions: (1) vertical velocity and acceleration are negligible; (2) pressure distribution is hydrostatic; (3) depth-averaged values are sufficient to describe properties which vary over flow depth; (4) the bottom slopes are small in both directions. The continuity and momentum equations (Khan and Chaudhry, 1992; Vreugdenhil, 1994; Yulistiyanto , 1997) are the following:

$$\frac{\partial h}{\partial t}+\frac{\partial Uh}{\partial x}+\frac{\partial Vh}{\partial y} = 0 \qquad (1)$$

$$\frac{\partial Uh}{\partial t}+\frac{\partial\left(U^2h+\tfrac{1}{2}gh^2\right)}{\partial x}+\frac{\partial UVh}{\partial y} = gh\left(S_{0x}-S_{fx}\right)+\frac{\partial}{\partial x}\left(\frac{h}{\rho}T_{xx}\right)+\frac{\partial}{\partial y}\left(\frac{h}{\rho}T_{xy}\right) \qquad (2)$$

$$\frac{\partial Vh}{\partial t}+\frac{\partial\left(V^2h+\tfrac{1}{2}gh^2\right)}{\partial y}+\frac{\partial UVh}{\partial x} = gh\left(S_{0y}-S_{fy}\right)+\frac{\partial}{\partial x}\left(\frac{h}{\rho}T_{yx}\right)+\frac{\partial}{\partial y}\left(\frac{h}{\rho}T_{yy}\right) \qquad (3)$$

where h is the flow depth and g is the acceleration of gravity; U and V are the depth-averaged velocity components, defined as:

$$U = \frac{1}{h}\int_o^h \bar{u}(z)\,dz \quad \text{and} \quad V = \frac{1}{h}\int_o^h \bar{v}(z)\,dz \tag{4}$$

where $\bar{u}(z)$ and $\bar{v}(z)$ are the local time-averaged velocity components.
The depth- averaged effective stresses in vertical planes are defined as:

$$T_{xx} = \frac{1}{h}\int_o^h \rho\left[2\nu\frac{\partial \bar{u}}{\partial x} - \overline{u'u'} - U'U'\right]dz \tag{5}$$

$$T_{xy} = T_{yx} = \frac{1}{h}\int_o^h \rho\left[\nu\left(\frac{\partial \bar{u}}{\partial y} + \frac{\partial \bar{v}}{\partial x}\right) - \overline{u'v'} - U'V'\right]dz \tag{6}$$

$$T_{yy} = \frac{1}{h}\int_o^h \rho\left[2\nu\frac{\partial \bar{v}}{\partial y} - \overline{v'v'} - V'V'\right]dz \tag{7}$$

where ρ and ν are respectively the density and the kinematic viscosity of the fluid; u' and v' are the turbulent velocity fluctuations; the local time-averaged velocity components $\bar{u}(z)$ and $\bar{v}(z)$, are distributed over the flow depth : the deviations from the depth-averaged values, eqs. (4) are expressed as:

$$U' = (\bar{u} - U) \quad \text{and} \quad V' = (\bar{v} - V) \tag{8}$$

and correspond to dispersion stresses.

DIFFUSION-DISPERSION TERMS

Diffusion-Dispersion terms consist of three types of effective stresses, namely molecular viscosity, turbulent and "dispersion" stresses. At sufficiently high Reynolds-number flow, the viscosity stresses can be neglected compared to the turbulent stresses. Using the Boussinesq's eddy-viscosity concept, the turbulent stresses are assumed to be proportional to the mean-velocity gradients. They may be expressed as (Yulistiyanto, at. al., 1998):

$$T'_{xx} = \rho\overline{\nu_t}\,2\frac{\partial U}{\partial x}, \quad T'_{xy} = T'_{yx} = \rho\overline{\nu_t}\left(\frac{\partial U}{\partial y} + \frac{\partial V}{\partial x}\right), \quad T'_{yy} = \rho\overline{\nu_t}\,2\frac{\partial V}{\partial y} \tag{9}$$

The "dispersion" stresses appear from the depth-integration of the advective

$$M_x = \int_o^h U'C'dz = \left(-K_{xx}\frac{\partial C}{\partial x} - K_{xy}\frac{\partial C}{\partial y}\right)h \tag{10a}$$

$$M_y = \int_o^h V'C'dz = \left(-K_{yx}\frac{\partial C}{\partial x} - K_{yy}\frac{\partial C}{\partial y}\right)h \tag{10b}$$

where C is a depth-averaged concentration and $C'(z)$ is the deviation of the local concentration from that mean value. The coefficients,- K_{ij}, expressing the diffusive property of the velocity distribution, can be calculated from the velocity deviation components, U' and V', and from the vertical eddy diffusivity, ε_{tz}, or :

$$K_{xx} = -\frac{1}{h}\int_o^h U'\left(\int_o^z \frac{1}{\varepsilon_{tz}}\int_o^z U'\,dz\,dz\right)dz \qquad K_{xy} = -\frac{1}{h}\int_o^h U'\left(\int_o^z \frac{1}{\varepsilon_{tz}}\int_o^z V'\,dz\,dz\right)dz$$

$$K_{yx} = -\frac{1}{h}\int_o^h V'\left(\int_o^z \frac{1}{\varepsilon_{tz}}\int_o^z U'\,dz\,dz\right)dz \qquad K_{yy} = -\frac{1}{h}\int_o^h V'\left(\int_o^z \frac{1}{\varepsilon_{tz}}\int_o^z V'\,dz\,dz\right)dz \tag{11}$$

Assuming the momentum flux is analogous to the mass flux, we can replace the concentration, C', by the momentum transfer components, $-\rho U'$ and $-\rho V'$, the dispersion stresses can now be re-written:

$$T^d_{xx} = \rho\left(K_{xx}\frac{-U}{-x} + K_{xy}\frac{-U}{(1353x-}\right), \qquad T^d_{xy} = \rho\left(K_{yx}\frac{\partial V}{\partial \xi} + K_{yy}\frac{\partial}{\partial}\right)$$

$$T^d_{yx} = \rho\left(K_{xx}\frac{\partial V}{\partial x} + K_{xy}\frac{\partial V}{\partial y}\right), \qquad T^d_{yy} = \rho\left(K_{yx}\frac{\partial V}{\partial x} + K_{yy}\frac{\partial V}{\partial y}\right) \tag{12}$$

However, for two-dimensional flow, the velocity distribution is generally only known along streamlines in such a way that re-writing (11) into a new set of coordinates (s, n) - respectively parallel and normal to the mean streamline - may be useful:

$$K_{ss} = -\frac{1}{h}\int_o^h U'_s\left(\int_o^z \frac{1}{\varepsilon_{tz}}\int_o^z U'_s\,dz\,dz\right)dz \qquad K_{sn} = -\frac{1}{h}\int_o^h U'_s\left(\int_o^z \frac{1}{\varepsilon_{tz}}\int_o^z V'_n\,dz\,dz\right)dz \tag{13}$$

The dispersion coefficients K_{xx}, K_{xy}, K_{yx} and K_{yy} are related to the streamline-oriented coefficients K_{ss}, K_{sn}, K_{ns} and K_{nn} by the following transformation (Yulistiyanto, 1997):

$$K_{xx}=K_{ss}\cos^2\theta - K_{sn}\sin\theta\cos\theta - K_{ns}\sin\theta\cos\theta + K_{nn}\sin^2\theta \quad (14a)$$

$$K_{xy}=K_{ss}\sin\theta\cos\theta + K_{sn}\cos^2\theta - K_{ns}\sin^2\theta - K_{nn}\sin\theta\cos\theta \quad (14b)$$

$$K_{yx}=K_{ss}\sin\theta\cos\theta - K_{sn}\sin^2\theta + K_{ns}\cos^2\theta - K_{nn}\sin\theta\cos\theta \quad (14c)$$

$$K_{yy}=K_{ss}\sin^2\theta + K_{sn}\sin\theta\cos\theta + K_{ns}\sin\theta\cos\theta + K_{nn}\cos^2\theta \quad (14d)$$

where θ is the angle between the streamline direction and the x-coordinate.

For use of eqs. (13), assumptions about the velocity profiles are needed. The velocity along the streamline is assumed to be given by a logarithmic distribution, such as (Rozovskii , 1957, p.33):

$$\bar{u}_s(\eta)=U_s+\frac{u_*}{\kappa}(1+\ln\eta) \quad (15)$$

where $\eta=z/h$ is the relative depth, κ is the von Karman constant and u_* is the friction velocity. Using this mean velocity distribution and assuming that both components vanish at the bottom, Rozovskii (1957, p.41 and p.54) derived a formula for the transverse velocity profile for a smooth bed :

$$\bar{v}_n(\eta)=\frac{h\,U_s}{\kappa^2\,r}\left\{F_1(\eta)-\frac{u_*}{\kappa U_s}F_2(\eta)\right\} \quad (16a)$$

and for a rough bed :

$$\bar{v}_n(\eta)=\frac{h\,U_s}{\kappa^2\,r}\left\{F_1(\eta)-\frac{u_*}{\kappa U_s}\left[F_2(\eta)+0.8(1+\ln\eta)\right]\right\} \quad (16b)$$

where $F_1(\eta)$ and $F_2(\eta)$ are functions of the relative depth η:

$$F_1(\eta)=\int_0^\eta\frac{2\ln(\eta)}{\eta-1}d\eta \quad \text{and} \quad F_2(\eta)=\int_0^\eta\frac{\ln^2(\eta)}{\eta-1}d\eta \quad (17)$$

The radius of the mean streamline r, can be obtained from the known values of U and V, since the curvature is given by:

$$\frac{1}{r}=\frac{d^2y/dx^2}{\left[1+\left(dy/dx\right)^2\right]^{3/2}}=\frac{\frac{d(\tan\theta)}{dx}}{\left[1+\tan^2\theta\right]^{3/2}} \quad (18)$$

It is now possible to write the lateral momentum exchange, corresponding to the two last terms of eqs. (2) and (3):

$$\frac{\partial}{\partial x}\left(\frac{h}{\rho}T_{xx}\right)+\frac{\partial}{\partial y}\left(\frac{h}{\rho}T_{xy}\right)=\frac{\partial}{\partial x}\left[(2\bar{v}_t+K_{xx})h\frac{\partial U}{\partial x}+K_{xy}h\frac{\partial U}{\partial y}\right] + \frac{\partial}{\partial y}\left[K_{yx}h\frac{\partial U}{\partial x}+(\bar{v}_t+K_{yy})h\frac{\partial U}{\partial y}+\bar{v}_t h\frac{\partial V}{\partial x}\right] \quad (19)$$

$$\frac{\partial}{\partial x}\left(\frac{h}{\rho}T_{yx}\right)+\frac{\partial}{\partial y}\left(\frac{h}{\rho}T_{yy}\right)=\frac{\partial}{\partial x}\left[(\bar{v}_t+K_{xx})h\frac{\partial V}{\partial x}+K_{xy}h\frac{\partial V}{\partial y}+\bar{v}_t h\frac{\partial U}{\partial y}\right] + \frac{\partial}{\partial y}\left[K_{yx}h\frac{\partial V}{\partial x}+(2\bar{v}_t+K_{yy})h\frac{\partial V}{\partial y}\right] \quad (20)$$

FINITE-DIFFERENCE APPROXIMATION

The system of differential equations (1)-(3) is too complex to be solved by analytical predictor-corrector scheme (Fletcher, 1988, p.404).

The scheme is second-order accurate in space and time and is also able to capture shocks (Ballamudi and Chaudhry, 1992). The schematic definition of this discretization scheme and the finite-difference approximations for the first- and second-order partial derivatives are given elsewhere (Yulistiyanto, 1997).

Forward finite-differences, using the known variables, are used for approximating the spatial partial differential terms in the predictor step while *backward* finite-differences, using the predicted variables, are used in the corrector step. Forward and backward finite-differences are now exchanged for the next predictor-corrector cycle to avoid the directional bias of the scheme.

For the steady flow, these processes are repeated until the convergence to a steady state condition is reached.

With some simplifications, it was demonstrated (Yulistiyanto, 1997) that the MacCormack scheme for the 2-D convection-diffusion equation is stable, if the following condition is satisfied :

$$\Delta t < C_n \frac{1}{\frac{(U+\sqrt{gh})_{i,j}}{\Delta x} + \frac{(V+\sqrt{gh})_{i,j}}{\Delta y} + \frac{2(K_{xx}+\bar{v}_t)}{\Delta x^2} + \frac{2(K_{xy}+\bar{v}_t)}{\Delta y^2}} \qquad (21)$$

where C_n is the desired Courant number, which should be: $C_n \leq 1.0$.

BOUNDARY CONDITIONS

The initial condition are defined according to uniform flow: the corresponding *U, V,* and *h* values are imposed at all grid points in the initial time step. In this present study, three types of boundaries are encountered: the wall boundaries, the upstream and the downstream (open) boundary. The finite-difference scheme is valid for the interior grid points. At the boundaries, some terms of these equations become indefinite. Therefore, to determine conditions at the boundaries, the mirror conditions (Roache, 1972) are used. The free-slip condition is used along the walls. The direction of the flow is determined in such a way that the normal velocity of each point at the wall is zero. The upstream or inflow boundary is an open boundary where flow enters the computational domain. Two-directional discharges, $Q_x = Q_x(t)$ and $Q_y = Q_y(t)$, are given and the other parameter, *h*, is found by solving the difference equation based on the characteristic form of the flow equations. In the present simulation, the transverse velocity is prescribed equal to zero and the discharge is constant with the time; the flow depth is calculated by the characteristic boundary procedure (Streeter ,1971, pp.682-690, Graf and Altinakar, 1996). Since a fixed grid is being considered, the method of characteristics needs an interpolation procedure. The downstream condition generally imposes the water depth $h = h(t) = h_{down}$ and is handled in a similar way.

NUMERICAL RESULTS

The numerical simulation was done for two test runs; the hydraulic parameters are given in Table 1 and Fig. 1, where the symbols are explained. On the same figure is also shown the limited domains, used for the grid visualization and for the velocity visualization, according to Fig. 2.

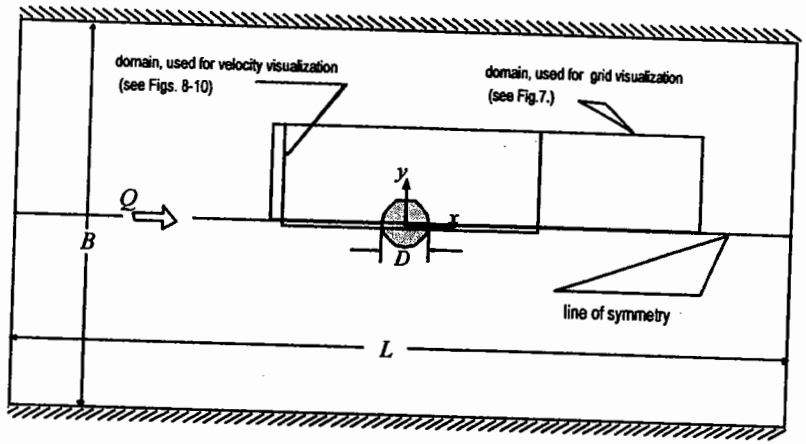

Fig. 1. Computational domain of the numerical simulation

For test 1 and 2, the size of this computational domain, *B* and *L*, were selected on the basis of the actual geometry of the laboratory channel, where measurement are performed.

Table 1 Uniform flow variables and channel parameters.

Test	cylinder		channel : uniform flow							
	D [m]	Re_D 10^5 [-]	B/L [m/m]	Q [m^3/s]	S_0 10^{-4}[-]	n [$m^{-1/3}s$]	U [m/s]	V [m/s]	h [m]	
1	0.22	1.48	2.0/4.0	0.248	6.25	0.012	0.67	0.000	0.185	calculated
				0.248	6.25	0.012	0.67	0.016	0.185	measured
2	0.22	0.95	2.0/4.0	0.149	2.80	0.012	0.43	0.00	0.173	calculated
				0.149	2.80	0.012	0.43	0.01	0.173	measured

The computation was carried out with a non-uniform grid (see Fig. 2). The size of the grid is smaller close to the cylinder, in order to get more information on flow near the cylinder. The cell numbers of 80 in the *x*-direction and 60 in the *y*-direction were used in the computation. Distance intervals, Δx and Δy, have a minimum and a maximum value of 6.6 mm and 106.6 mm for test 1 and test 2, respectively. The time interval, Δt, is limited by the stability of the scheme (21), and is restricted by the Courant number, which was set for all the test equal to $C_n = 0.667$ (another Courant number, $C_n = 0.85$, was also used in the numerical simulation; the scheme remained stable) .

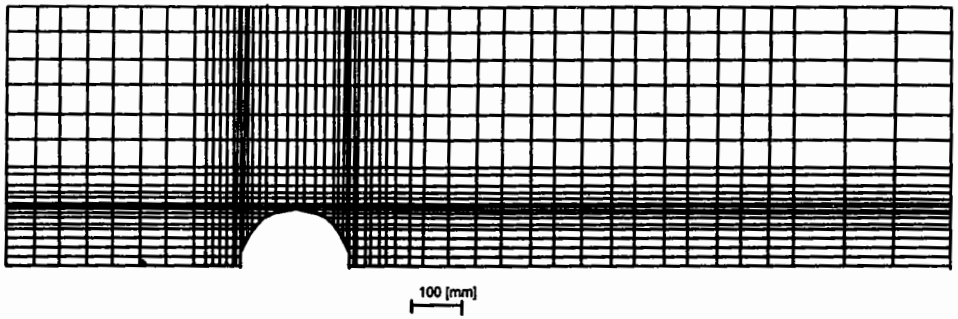

Fig. 2. Partial domain, showing the grid points

The results of the numerical simulations of the flow field are given in Fig. 3 for test 1, and in Fig. 4 for test 2. The boundary conditions at the channel inlet and outlet are situated far enough from the cylinder, thus they do not influence the condition of the flow around the cylinder. The inflow discharge, Q, is maintained constant with time. The water depth at the channel outlet, h_{down} is also maintained constant. Along the wall boundaries, consisting of the two vertical side walls and the perimeter of the cylinder, the normal velocity is zero with a perfect slip condition.

The governing equations (1-3), describe unsteady flow, however by applying steady conditions at both upstream and downstream boundaries, a convergence to steady state is obtained. The simulation reaches this steady state after 3 sec simulated time from the beginning of the computation. Simulations were stopped at t = 4.2 sec for test 1and at t = 4.4 sec for test 2.

The relative importance of each term in the momentum equations (2-3), was also investigated (Yulistiyanto ,1997, Appendix E). It provided interesting detailed information: the inertia terms are of dominating importance; the slope terms are insignificant; the diffusion-dispersion terms take important values.

The numerical simulation allowed also to obtain information about the change in the flow depth, $h(x, y)$, due to the presence of the cylinder (Figs. 5). The typical bow wave, having the highest superelevation in front of the cylinder – i.e.: $h_s - h_\infty \approx U^2/2g$ – is observed. Its level decreased considerably going around the cylinder, becoming the lowest depression at the rear of the cylinder.

Conclusively, it can be said, that the depth-averaged simulation of the flow around a cylinder gives results, which are to be considered reasonable in the light of the existing literature.

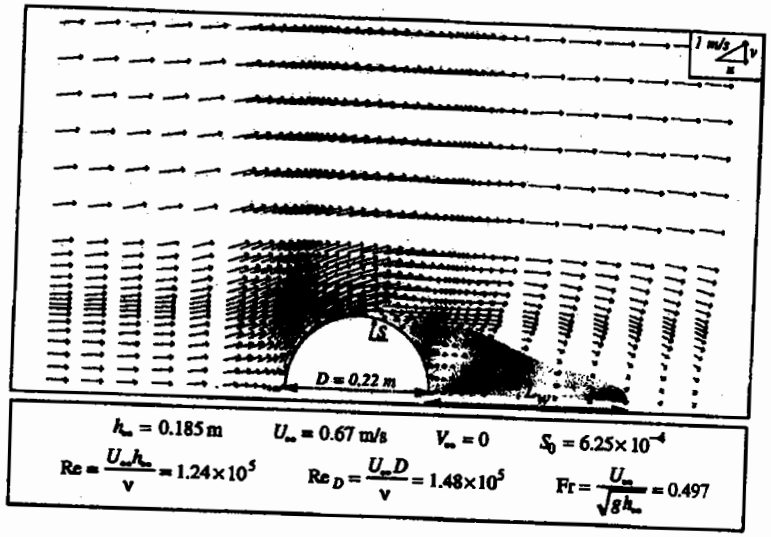

Fig. 3 Numerical Simulation of Flow Field, for Test 1, for Steady State Condition at t=4,2 s.

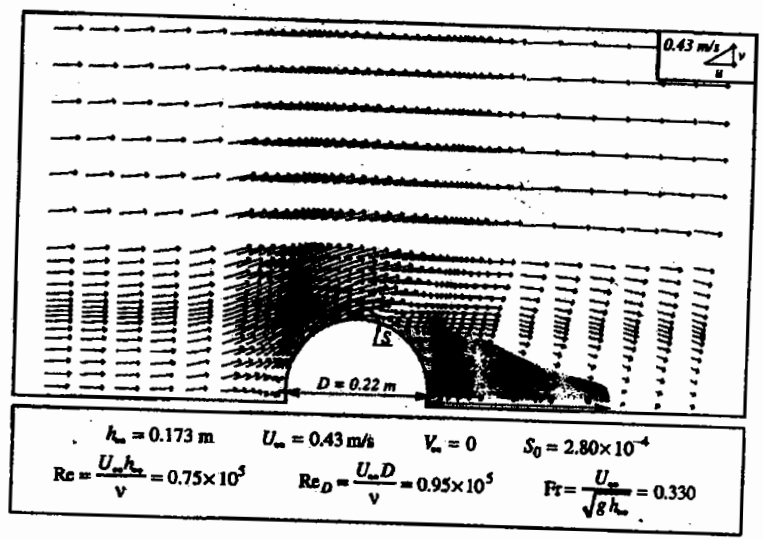

Fig. 4 Numerical Simulation of Flow Field, for Test 2, for Steady State Condition at t=4,4 s.

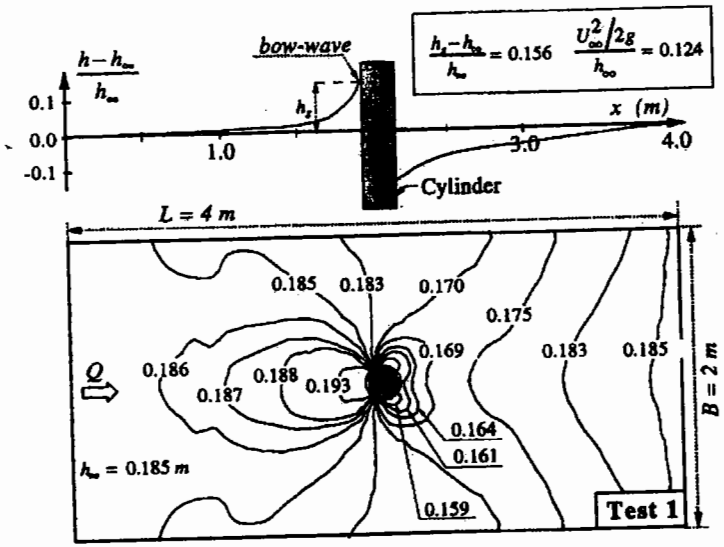

Fig. 5 Topography (Simulation) of Flow Depth for Test 1.

COMPARISON WITH EXPERIMENTAL RESULTS

In order to check the numerical simulations, two runs (test 1 and test 2) were performed (Yulistiyanto, 1997). The velocity measurements are done with an Acoustic Doppler Velocity Profiler (ADVP). The vertical distribution of the velocity in all three directions was measured, however only velocities in the longitudinal, u, and transversal, v, directions are used in the comparison with the numerical simulation. These measurements are done along 5 lines radiating from the cylinder, under the angles of 0°, 45°, 90°, 157.5° and 180° for test 1, and under the angles of 0°, 45°, 90°, 135° and 180° for test 2; for each line, these measurements were performed at 8 to 12 positions. At each of them, the flow depth was also measured. From the vertical mean-velocity distributions, the depth-averaged velocities, U and V, in the flow field around the cylinder were then calculated. These data are used to verify the applicability of the numerical model.

The velocity vectors resulting from the numerical simulation for test 1 and test 2 at steady state, together with the depth-averaged velocities from the experimental works, are shown in Figs. 6 and 7. The velocity vectors upstream from the cylinder and along the sides are in reasonably good agreement. Nevertheless very close to the cylinder, the simulation sometimes underpredicts the velocities. Downstream from the cylinder, where the flow structure is complex (see Figs. 3 and 4), the agreement is satisfactory both inside and outside the cylinder wake.

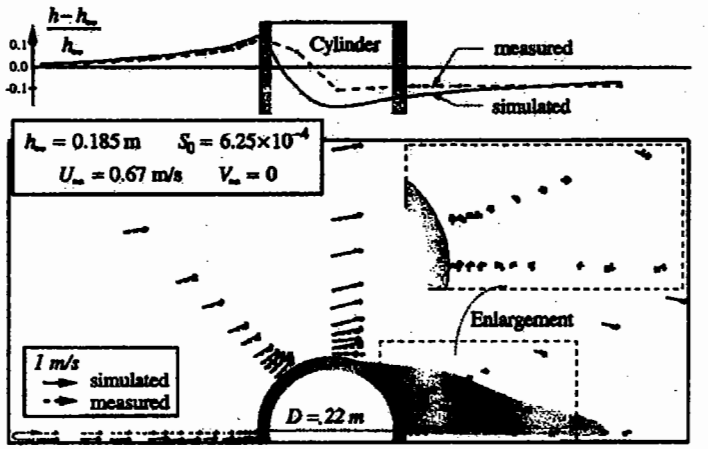

Fig. 6 Comparison between Experimental and Simulation Flow Field, for Test 1.

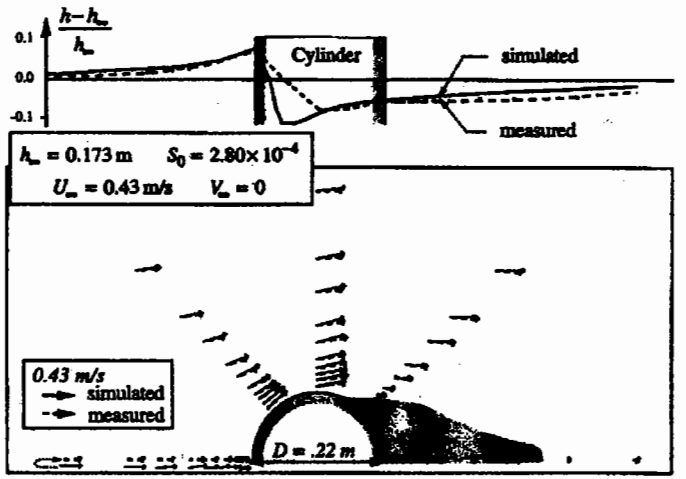

Fig. 7 Comparison between Experimental and Simulation Flow Field, for Test 2.

The flow depths at the center line both upstream and downstream from the cylinder are also in good agreement, however on the circumference of the cylinder the simulated flow depths are smaller than the experimental ones. It must be commented that flow-depth measurements in the vicinity of the cylinder are not easy due to water-level fluctuations. The measured depth is thus rather an upper limit of the fluctuations than the averaged level which is very difficult to estimate. Despite using free-slip conditions along the walls and shallow-water equations, the agreement between experimental and numerical results is reasonably good. Taking into account dispersion

CONCLUSION

The Saint-Venant equations (1-3) for two-dimensional depth-averaged flow, including exchanges through vertical planes, were used to simulate flow around a cylinder positioned in an open channel. A special emphasis was placed in elaborating the diffusion-dispersion terms.

Numerical solutions were obtained using an explicit finite-difference scheme according to MacCormack, with appropriate boundary conditions. Two different cases, (see Table 1), were simulated, from which resulting flow fields are given in Figures 3 and 4. The expected flow alteration due to the presence of the cylinder is evident, notably the wake behind the cylinder. The simulated topography of the flow depths, (see Fig.5), showed clearly the existence of a bow-wave and the subsequent depression in the vicinity of the cylinder.

Laboratory experiments were performed in parallel for two cases. The comparison given in Fig. 6 and Fig. 7, between experimental data and simulated results is considered as being reasonably satisfactory, both for the flow fields and for the elevations. This shows that 2-D finite-difference modeling, including lateral momentum exchanges and dispersion terms without any parameter to be calibrated, is able to approach a relatively complex situation.

ACKNOWLEDGEMENTS

The author acknowledges the contributions from Prof. Dr. Yves Zech of UCL-Belgium, and from Prof. Dr. W. Graf of EPF Lausanne-Switzerland, for their constructive advises.

REFERENCES

Ballamudi, S. M. and Chaudhry, M. H. (1992) : "Computational of flows in open-channel transitions.", *Journal of Hydraulic Research* , vol. 30(no. 9), pp. 1145-1164.

Fennema, R. J. and Chaudhry, M. H. (1986): "Explicit numerical scheme for unsteady free-surface flows with shocks.", *Water Resources Research* , 22(13), pp. 1923-1930.

Fischer H.B., List E.J., Koh R.C.Y., Imberger J. and Brooks N. (1979) : *Mixing in inland and coastal Waters*, Academic Press, New York, USA

Fletcher C.A.J. (1988) : *Computational Techniques for Fluid Dynamics; Vol. 2*, Springer-Verlag, Berlin-Heidelberg-New York

Flokstra, C., (1977) : *The Closure Problem for Depth-Averaged Two-dimensional Flow*, Paper A106, 17th Intern. Assoc. for Hydraulics Research Congress, Baden-Baden, D

Graf W.H. and Altinakar M.S.(1996) : *Hydraulique fluviale;* Tome 2, Presses Polytechniques et Univ. Romandes, Lausanne, CH

Khan K.W. and Chaudhry M.H. (1992) : "Numerical Modeling of Flow around Spur Dikes", *Proc. fourth Int. Conf. on Hydraulic Engineering Software - Valence HYDROSOFT 92*, pp. 223-235, Computational Mechanics Publications, Southampton, UK

Roache P.J. (1972) : *Computational Fluid Dynamics*, Hermosa Publ., Albuquerque, New Mexico, USA

Rodi W. (1984) : *Turbulence Models and their Applications in Hydraulics*, IAHR publications, Delft, NL

Rozovskii I.L (1957) : *Flow of Water in Bends of Open Channels*, Israel Program for Scientific Translations, Jerusalem, I

Streeter V.L. (1971) : *Fluid mechanics*, fifth edition, International Student Edition, McGraw-Hill, Inc., New York, USA

Vreugdenhil, C.B. (1973) : *Secondary-flow Computations*, 15th Intern. Assoc. for Hydraulics Research Congress, Istambul, T

Vreugdenhil C.B. (1994) : *Numerical Methods for Shallow-Water Flow*, Kluwer Academic Publishers, Dordrecht, NL

Yulistiyanto B. (1997) : *Flow around a cylinder installed in a fixed-bed open channel* , PhD dissertation, No. 1631, Ecole Polytechnique Fédérale, Lausanne, CH.

Yulistiyanto B., Y. Zech, W.H. Graf (1998) : 'Flow around a cylinder : Shallow-water modeling with diffusion-dispersion, *Journal of Hydraulic Engineering*, ASCE, vol. 124 (no.4), pp. 419-429.